



This discussion paper is/has been under review for the journal Geoscientific Model Development (GMD). Please refer to the corresponding final paper in GMD if available.

Conservative interpolation between general spherical meshes

E. Kritsikis¹, M. Aechtner², Y. Meurdesoif³, and T. Dubos²

¹Laboratoire d'analyse, géométrie et applications, université Paris 13,
93430 Villetaneuse, France

²Laboratoire de météorologie dynamique, École polytechnique – IPSL,
91128 Palaiseau, France

³Laboratoire des sciences du climat et de l'environnement, CEA – IPSL,
91191 Gif sur Yvette, France

Received: 04 March 2015 – Accepted: 23 March 2015 – Published: 30 June 2015

Correspondence to: E. Kritsikis (krits@math.univ-paris13.fr)

Published by Copernicus Publications on behalf of the European Geosciences Union.

GMDD

8, 4979–4996, 2015

Conservative
interpolation between
general spherical
meshes

E. Kritsikis et al.

Title Page

Abstract

Introduction

Conclusions

References

Tables

Figures

◀

▶

◀

▶

Back

Close

Full Screen / Esc

Printer-friendly Version

Interactive Discussion



Abstract

An efficient, local, explicit, second-order, conservative interpolation algorithm between spherical meshes is presented. The cells composing the source and target meshes may be either spherical polygons or longitude–latitude quadrilaterals. Second-order accuracy is obtained by piecewise-linear finite volume reconstruction over the source mesh. Global conservation is achieved through the introduction of a supermesh, whose cells are all possible intersections of source and target cells. Areas and intersections are computed exactly to yield a geometrically exact method. The main efficiency bottleneck caused by the construction of the supermesh is overcome by adopting tree-based data structures and algorithms, from which the mesh connectivity can also be deduced efficiently.

The theoretical second-order accuracy is verified using a smooth test function and pairs of meshes commonly used for atmospheric modelling. Experiments confirm that the most expensive operations, especially the supermesh construction, have $O(N \log N)$ computational cost. The method presented is meant to be incorporated in pre- or post-processing atmospheric modelling pipelines, or directly into models for flexible input/output. It could also serve as a basis for conservative coupling between model components, e.g. atmosphere and ocean.

1 Introduction

Despite the simplicity and regularity of a spherical surface, there is no single ideal way to mesh it. Consequently, numerical methods formulated on the sphere, used for instance in weather forecasting and climate modelling, use a variety of meshes. For a long time spectral and finite-difference schemes have been using longitude–latitude meshes. However most recently developed methods use more flexible meshes like triangulations of the sphere and their Voronoi dual, or quadrangular meshes like the

GMDD

8, 4979–4996, 2015

Conservative interpolation between general spherical meshes

E. Kritsikis et al.

Title Page

Abstract

Introduction

Conclusions

References

Tables

Figures

◀◀

▶▶

◀

▶

Back

Close

Full Screen / Esc

Printer-friendly Version

Interactive Discussion



“cubed-sphere”. Such meshes avoid the polar singularity inherent to the longitude–latitude system (Williamson, 2007).

Different physical components like atmosphere, land, ice, ocean typically use distinct meshes. As they are coupled together interpolation between the various meshes is required. Furthermore the native model mesh may not be the most practical to perform post-processing and analysis of the simulations, and interpolating to a more convenient mesh can be desirable. Finally interpolation is a crucial building block of dynamic mesh adaptation, which enables a simulation to dynamically focus resolution where it is important, potentially saving orders of magnitude in computational costs. Although dynamic adaptivity is not a current practice in ocean/atmosphere modelling, there is a growing body of research to this end, and dynamic adaptivity may mature in the future. Meanwhile statically refined meshes are increasingly used, and there is a need to interpolate from/to such meshes.

In applications like climate modelling, it is often vital that some physical quantities be conserved, such as density, volume fractions or tracer concentrations. When interpolating fluxes between physical component coupled together, similar conservation constraints should be enforced. Failing to enforce these conservation properties may create spurious sources and sinks which, however small, may accumulate over time and overwhelm the physical trends. Therefore even if one uses a conservative discretisation method for the relevant PDEs, there is a need to ensure conservation in the interpolation step.

This paper describes a second-order conservative interpolation algorithm on the sphere. Our method improves over previously published work as follows:

- it is geometrically exact as defined and discussed in Ullrich et al. (2009), and unlike Jones (1999)
- it is not tied to a narrow class of meshes (e.g. Ullrich et al., 2009 which handles only cubed-sphere and lon-lat meshes): our method handles lon-lat meshes and arbitrary polygonal meshes, including the cubed-sphere, general triangulations

GMDD

8, 4979–4996, 2015

Conservative interpolation between general spherical meshes

E. Kritsikis et al.

Title Page

Abstract

Introduction

Conclusions

References

Tables

Figures



Back

Close

Full Screen / Esc

Printer-friendly Version

Interactive Discussion



and their Voronoi duals, which encompasses the vast majority of currently-used meshes

- it is local and explicit, unlike optimisation-based approaches (Farrell et al., 2009) which require an iterative solver. Therefore a small number of interpolation weights can be pre-computed and parallelism is facilitated.

Our method relies on the availability of a supermesh, i.e. a mesh which refines both the source and target meshes. Assuming that the supermesh is known, formulae for second-order conservative interpolation are derived in Sect. 2. Algorithms used to construct the supermesh are described in Sect. 3. Numerical experiments are conducted in Sect. 4 to verify the accuracy of the method when used with various pairs of spherical meshes, as well as the theoretical algorithmic complexity. A summary is given in Sect. 5.

2 Second-order conservative interpolation

The source and target meshes are sets of spherical cells S_i and T_j , each cell being either a spherical polygon or a lon-lat quadrilateral. The intersection $S_i \cap S_j$ (resp. $T_i \cap T_j$) for $i \neq j$ is either void, a shared vertex or a shared edge. The latter case defines neighboring cells. Both meshes are assumed to cover the whole sphere i.e. $\bigcup S_i = \bigcup T_j$.

Scalar functions are assumed to be described via their integrals over mesh cells. Indeed in most GCMs many if not all fields are treated in a finite-volume manner. The problem we wish to solve is, given the integrals f_i of a smooth function f on the source mesh, to obtain accurate estimates f'_j of the integrals on the target mesh, so that the total integral is preserved:

$$\sum_i f_i = \sum_j f'_j. \quad (1)$$

GMDD

8, 4979–4996, 2015

Conservative interpolation between general spherical meshes

E. Kritsikis et al.

Title Page

Abstract

Introduction

Conclusions

References

Tables

Figures

◀

▶

◀

▶

Back

Close

Full Screen / Esc

Printer-friendly Version

Interactive Discussion



Second-order accuracy will result from linear reconstructions on each S_i , assuming f has a bounded second derivative. To achieve conservation (Eq. 1), one introduces the supermesh $U_k = (S_i \cap T_j)_{i,j}$. The supermesh is such that any cell of both source and destination meshes is the union of cells of the supermesh. The problem comes down to finding approximations

$$f_k'' \approx \int_{U_k} f \quad \text{s. t.} \quad \sum_{U_k \subset S_i} f_k'' = f_i. \quad (2)$$

We want the approximation to be exact for a constant function. This property implies for the cell areas A_i, A_k :

$$A_i = \sum_{U_k \subset S_i} A_k. \quad (3)$$

To satisfy Eq. (3), all spherical areas are computed exactly (see Sect. 3.4). In the general case a piecewise linear reconstruction $\tilde{f} \in PC^1(S)$ of f over the source mesh is built and integrated by approximate quadrature over U_k , yielding f_k'' . We define the reconstruction as

$$\tilde{f}_i(x) = \bar{f}_i + g_i \cdot (x - C_i) \quad \text{for any } x \in \mathring{S}_i, \quad (4)$$

where $\bar{f}_i = f_i / A_i$ is the mean value of f over S_i , g_i is an approximation of the gradient of f on S_i and C_i is the centroid of S_i . The quadrature is defined as $f_k'' = A_k \tilde{f}(C_k)$. It follows that

$$\forall i, \sum_{U_k \subset S_i} f_k'' = \sum_{U_k \subset S_i} A_k \bar{f}_i + \sum_{U_k \subset S_i} A_k g_i \cdot (C_k - C_i) \quad (5)$$

$$= f_i + g_i \cdot \sum_{U_k \subset S_i} A_k C_k - A_i g_i \cdot C_i, \quad (6)$$

in view of Eq. (3), which gives two necessary orthogonality conditions for Eq. (2) to hold:

GMDD

8, 4979–4996, 2015

Conservative interpolation between general spherical meshes

E. Kritsikis et al.

Title Page

Abstract

Introduction

Conclusions

References

Tables

Figures

◀◀

▶▶

◀

▶

Back

Close

Full Screen / Esc

Printer-friendly Version

Interactive Discussion



$$- \forall i, g_i \cdot C_i = 0,$$

$$- \forall i, g_i \cdot \sum_{U_k \subset S_i} A_k C_k = 0$$

By computing first the barycenters C_k of the supermesh cells U_k , then obtaining from them the barycenters of the source cells as $C_i = N(\sum_{U_k \subset S_i} A_k C_k)$, where $N(C) = C/\sqrt{C \cdot C}$, the two above conditions become equivalent. To satisfy them, a first-order estimate \tilde{g}_i of the gradient is orthogonalized with respect to C_i , yielding g_i . Since the orthogonality condition is satisfied by the exact gradient, this orthogonalization entails no loss of accuracy. The \tilde{g}_i are computed by the Gauss formula on a neighborhood of S_i , that is the polygon Σ_i joining the centroids of neighbouring elements (Tomita et al., 2001). Indeed as

$$\int_{V_i} \nabla f = \int_{\partial \Sigma_i} (f - \bar{f}_i) n ds, \quad (7)$$

with $\partial \Sigma_i$ the boundary of Σ_i and n the outward normal to Σ_i , we set

$$\tilde{g}_i = \frac{1}{A(\Sigma_k)} \sum_{\substack{S_i \cap S_j \cap S_k \neq \emptyset \\ i, j, k \text{ distinct}}} \left(\frac{\bar{f}_j + \bar{f}_k}{2} - \bar{f}_i \right) C_j \times C_k \quad (8)$$

where each pair j, k of neighbours appears only once, so that the triangle $C_i C_j C_k$ is counter-clockwise. In Eq. (8), subtracting \bar{f}_i guarantees that a constant field has a zero gradient.

GMDD

8, 4979–4996, 2015

Conservative interpolation between general spherical meshes

E. Kritsikis et al.

Title Page

Abstract

Introduction

Conclusions

References

Tables

Figures

◀

▶

◀

▶

Back

Close

Full Screen / Esc

Printer-friendly Version

Interactive Discussion



3 Spherical supermesh

3.1 Intersection between a pair of cells

We describe here how, given two cells C and C' , their intersection U is obtained. The unit sphere is represented as the surface $x^2 + y^2 + z^2 = 1$ in Cartesian coordinates. Intersection points between all pairs of edges of C and C' are computed by representing small and great circles as the intersection of the unit sphere with a plane. For great circles, this plane contains the origin, while it does not for small circles. Among the resulting segments, those which are inside either C or C' are collected and ordered counter-clockwise to form the boundary of U . Notice that U is allowed to have several connected components, in which case as many supermesh cells are created.

3.2 Fast search of potential intersectors

Constructing the supermesh requires in principle to compute the intersection between all S_i and T_j . Assuming both meshes have $O(N)$ cells, this brute-force approach has a quadratic algorithmic complexity $O(N^2)$. However in fact most intersections are empty. Moreover cells of the source and destination meshes can be grouped hierarchically in sets with mostly empty mutual intersections. Exploiting this fact, as described below, yields fast search algorithms and is crucial to attain $O(N \log N)$ algorithmic complexity.

The fast search algorithm takes as input a mesh and a spherical circle. It yields a list of cells in the mesh that potentially lie partly or totally inside the circle. The algorithm guarantees that all cells of the mesh that actually lie partly or totally in the circle are in the list. Some of those cells may in fact lie outside the circle, although the algorithm is designed to keep their number to a minimum.

In order to yield $O(N \log N)$ complexity, a bounding circle is computed for each cell and these circles are inserted sequentially into a similarity-search tree, or SS-tree (White and Jain, 1996), which grows progressively starting from an empty tree with a single root node. During this process, each node of the tree has its own bounding

Conservative interpolation between general spherical meshes

E. Kritsikis et al.

Title Page

Abstract

Introduction

Conclusions

References

Tables

Figures

◀◀

▶▶

◀

▶

Back

Close

Full Screen / Esc

Printer-friendly Version

Interactive Discussion



of the meshes. Indeed to reconstruct the connectivity of, say, the source mesh, it is sufficient to apply the previous algorithm to the source mesh and a source cell. This connectivity is required when computing the gradient \tilde{g}_j . Therefore our method works in circumstances where mesh connectivity is not readily available, for instance when reading data from NetCDF files following the NetCDF-CF convention (<http://cfconventions.org/>).

3.4 Supermesh cell area and barycenter

Supermesh cell edges are an arbitrary mix of small and great circle segments. To compute their area, we represent them as a combination of spherical triangles and surfaces enclosed by a small circle segment and a great circle segment with the same endpoints, possibly counted negatively. A similar approach is used for barycenters.

An accurate treatment of small circle segments is crucial for accuracy on reduced latitude–longitude grids (Purser, 1998). Indeed for such grids the cells close to the poles have strongly curved boundaries and approximations that conflate a small arc and the great arc with the same endpoints fail to deliver second-order accuracy (not shown).

4 Results

In this section we verify the accuracy and efficiency of the method, encompassing several types of meshes: latitude–longitude, triangular, polygonal dual and cubed-sphere (see Fig. 2). Computations were done on an Intel P8700 processor @2.53 GHz with 4 GB RAM.

4.1 Meshes

All meshes whose cell edges are an arbitrary mix of great and small spherical arcs are supported. This includes standard and skipped latitude–longitude meshes, cubed-

sphere meshes, triangulations and general polygonal meshes. Figure 2 shows meshes that we specifically use for the tests presented below:

- standard longitude–latitude meshes where the zonal and meridional resolution are equal at the Equator and the pole is a vertex,
- their skipped variant, where the number of cells along a parallel varies, starting at 4 around the pole and doubling to keep the zonal cell size less than twice the meridional cell size (Purser, 1998),
- cubed-sphere meshes (Sadourny, 1972),
- triangular-icosahedral meshes and their hexagonal-pentagonal Voronoi duals (Sadourny et al., 1968),
- variable-resolution variants of the latter obtained by applying a Schmidt transform to each vertex (Guo and Drake, 2005).

4.2 Accuracy

Interpolation between various pairs of meshes is applied to the smooth field $2 + xy$. The input data is obtained by evaluating this function at source cell barycenters G_j . The global conservation property (Eq. 1) is satisfied within round-of error (not shown). Interpolation error is evaluated by evaluating the test function at destination cell barycenters and comparing to the interpolated value $\bar{f}_j = f_j/A_j$:

$$\varepsilon_p = \left(\frac{1}{4\pi} \sum A_j \left\| \bar{f}_j - f(G_j) \right\|^p \right)^{1/p}$$

$$\varepsilon_\infty = \max_j \left\| \bar{f}_j - f(G_j) \right\|$$

When using a piecewise-constant reconstruction on the source mesh, interpolation error is expected to be proportional to the local gradient of the test function and to

Conservative interpolation between general spherical meshes

E. Kritsikis et al.

Title Page

Abstract

Introduction

Conclusions

References

Tables

Figures

◀

▶

◀

▶

Back

Close

Full Screen / Esc

Printer-friendly Version

Interactive Discussion



the cell size (largest of source and target mesh sizes). When using a piecewise-linear reconstruction, interpolation error is expected to be proportional to the local second derivatives of the test function and to the squared cell size.

We first consider remapping between pairs of uniform-resolution meshes of comparable resolution h ranging from 0.01 (a few hundred thousand cells) to 0.1 (a few thousand cells). Figure 3 shows the maximum (L^∞) and root-mean-square (L^2) interpolation error, as a function of a global characteristic cell size h defined as the average of the local cell sizes, themselves defined as the side-length of a square with same area A ($h = \sqrt{A}$). Scaling of both errors confirms that the expected first order (left) and second-order (right) accuracy is achieved.

An application to variable-resolution icosahedral-hexagonal meshes is shown in Fig. 4. The remapping is performed between two such meshes. The source mesh is everywhere about 25 % finer than the destination mesh while the resolution of each single mesh spans about a decade. As expected, the local error is found to be bounded $O(h^2)$ with h the local mesh size defined here as the square root of the destination cell area.

4.3 Efficiency

Figure 5 shows the computation time of a second-order remapping from a uniform resolution icosahedral-hexagonal mesh to a regular latitude–longitude mesh vs. the number N of elements of the meshes. Total time is decomposed according to the different steps of the algorithms. Since the remapping is a linear operator, it can be expressed in terms of weights forming a sparse matrix. These weights are typically pre-computed for repeated later use. The cost of computing intersections, gradients (only for second order) and weights is linear in the number of elements. Construction of the SS-tree has the theoretical complexity of $O(N \log N)$ (dashed line).

The overall computational cost is dominated by the computation of intersections and therefore close to linear. Extrapolating those curves suggests that for any imaginable

Conservative
interpolation between
general spherical
meshes

E. Kritsikis et al.

Title Page

Abstract

Introduction

Conclusions

References

Tables

Figures



Back

Close

Full Screen / Esc

Printer-friendly Version

Interactive Discussion



problem size the SS-tree will not require more computational resources than the computation of intersections, which has $O(N)$ complexity.

5 Conclusions

A local, explicit, second-order, conservative interpolation algorithm has been devised. The theoretical second-order accuracy has been verified using a smooth test function and pairs of meshes covering most meshes commonly used for atmospheric modelling. The main efficiency bottleneck caused by the construction of the supermesh has been overcome by adopting tree-based data structures and algorithms, from which the mesh connectivity can also be deduced efficiently. Experiments confirm a $O(N \log N)$ computational cost of the most expensive operations, especially the supermesh construction.

Cartesian curvilinear meshes are not covered by this work. Covering such meshes commonly used for ocean modelling requires essentially adapting the detailed computation of intersections. Higher-order interpolations, or vector interpolations can also easily be incorporated. This is left for future work.

Although the present sequential method is fast enough to be included as is into pre- or post-processing pipelines, further efficiency gains can be obtained by parallelizing it. The least parallel part of the algorithm is the SS-tree construction. Work is under way to parallelize this step, using again tree approaches to distribute and balance the workload, and will hopefully be presented separately.

Acknowledgements. E. Kritsikis and M. Aechtner acknowledge support by the ICOMEX project.

References

Farrell, P., Piggott, M., Pain, C., Gorman, G., and Wilson, C.: Conservative interpolation between unstructured meshes via supermesh construction, *Comput. Method. Appl. M.*, 198, 2632–2642, 2009. 4982

Conservative interpolation between general spherical meshes

E. Kritsikis et al.

Title Page

Abstract

Introduction

Conclusions

References

Tables

Figures



Back

Close

Full Screen / Esc

Printer-friendly Version

Interactive Discussion



- Guo, D. X. and Drake, J. B.: A global semi-Lagrangian spectral model of the shallow water equations with variable resolution, *J. Comput. Phys.*, 206, 559–577, 2005. 4988
- Jones, P.: First- and second-order conservative remapping schemes for grids in spherical coordinates, *Mon. Weather Rev.*, 127, 2204–2210, 1999. 4981
- 5 Purser, R.: Non-standard grids., *Proc. Seminar on Recent Developments in Numerical Methods for Atmospheric Modelling*, Reading, UK, ECMWF, 44–72, 1998. 4987, 4988
- Sadourny, R.: Conservative finite-difference approximations of the primitive equations on quasi-uniform spherical grids, *Mon. Weather Rev.*, 100, 136–144, 1972. 4988
- Sadourny, R., Arakawa, A. K. I. O., and Mintz, Y. A. L. E.: Integration of the nondivergent
- 10 barotropic vorticity equation with an icosahedral-hexagonal grid for the sphere, *Mon. Weather Rev.*, 96, 351–356, 1968. 4988
- Tomita, H., Tsugawa, M., Satoh, M., and Goto, K.: Shallow water model on a modified icosahedral geodesic grid by using spring dynamics, *J. Comput. Phys.*, 174, 579–613, 2001. 4984
- Ullrich, P. A., Lauritzen, P. H., and Jablonowski, C.: Geometrically Exact Conservative Remapping (GECORE): regular latitude–longitude and cubed-sphere grids, *Mon. Weather Rev.*, 137, 1721–1741, 2009. 4981
- 15 White, D. and Jain, R.: Similarity indexing with the SS-tree, in: *Proceedings of the Twelfth International Conference on Data of Conference*, New Orleans, LA, 26 February–1 March 1996, 516–523, 1996. 4985
- 20 Williamson, D. L.: The Evolution of Dynamical Cores for Global Atmospheric Models, *J. Meteorol. Soc. Jpn.*, 85B, 241–269, 2007. 4981

Conservative interpolation between general spherical meshes

E. Kritsikis et al.

Title Page

Abstract

Introduction

Conclusions

References

Tables

Figures

◀

▶

◀

▶

Back

Close

Full Screen / Esc

Printer-friendly Version

Interactive Discussion



Conservative interpolation between general spherical meshes

E. Kritsikis et al.

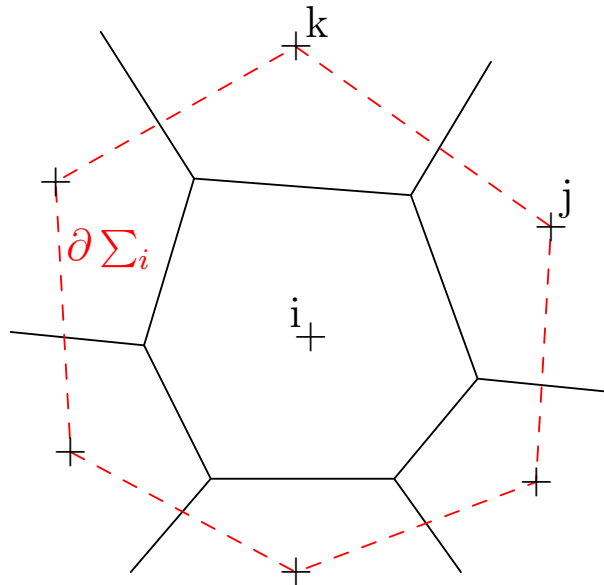


Figure 1. Gradient computation: Stokes formula is applied on the boundary $\partial\Sigma_i$ of the polygon surrounding cell i . The vertices of Σ_i are the barycenters of nearest-neighbour cells j, k, \dots

[Title Page](#)
[Abstract](#)
[Introduction](#)
[Conclusions](#)
[References](#)
[Tables](#)
[Figures](#)
[◀](#)
[▶](#)
[◀](#)
[▶](#)
[Back](#)
[Close](#)
[Full Screen / Esc](#)
[Printer-friendly Version](#)
[Interactive Discussion](#)


Conservative interpolation between general spherical meshes

E. Kritsikis et al.

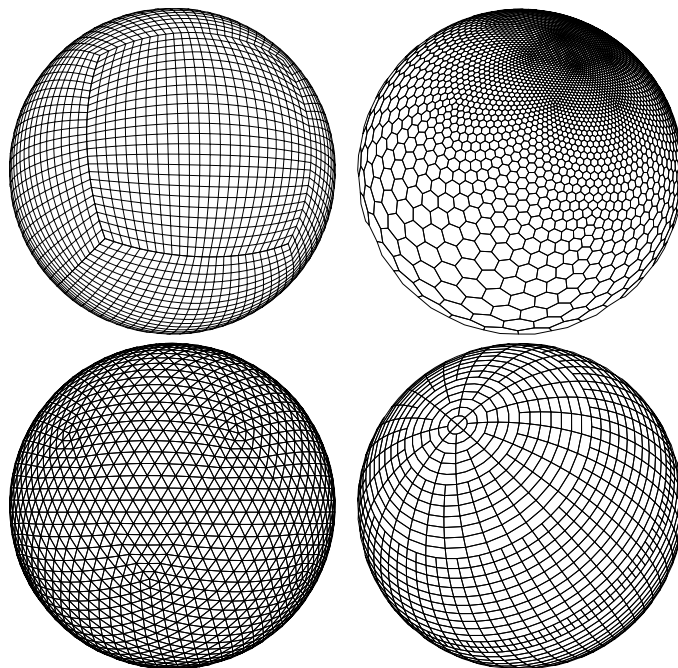
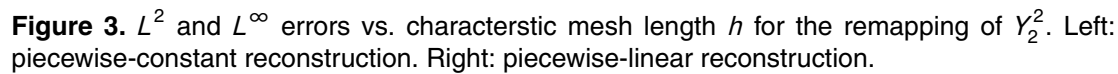


Figure 2. Different meshes are supported and have been tested: latitude–longitude, reduced latitude–longitude (bottom-right), triangular (bottom-left), cubed-sphere (top-left) and variable-resolution polygonal (top-right).

[Title Page](#)[Abstract](#)[Introduction](#)[Conclusions](#)[References](#)[Tables](#)[Figures](#)[Back](#)[Close](#)[Full Screen / Esc](#)[Printer-friendly Version](#)[Interactive Discussion](#)



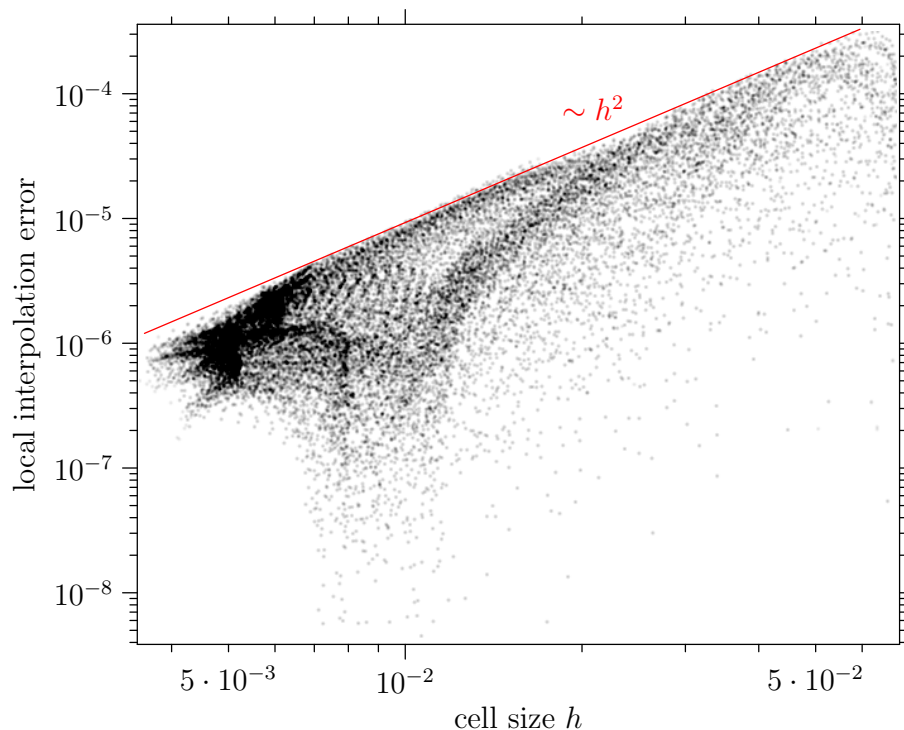


Figure 4. When mapping between non-uniform hexagonal meshes, the local error depends quadratically on the local resolution. Each dot represents a grid cell. The cell size h is computed as the square root of the cell area.

Conservative interpolation between general spherical meshes

E. Kritsikis et al.

Title Page

Abstract

Introduction

Conclusions

References

Tables

Figures

◀

▶

◀

▶

Back

Close

Full Screen / Esc

Printer-friendly Version

Interactive Discussion

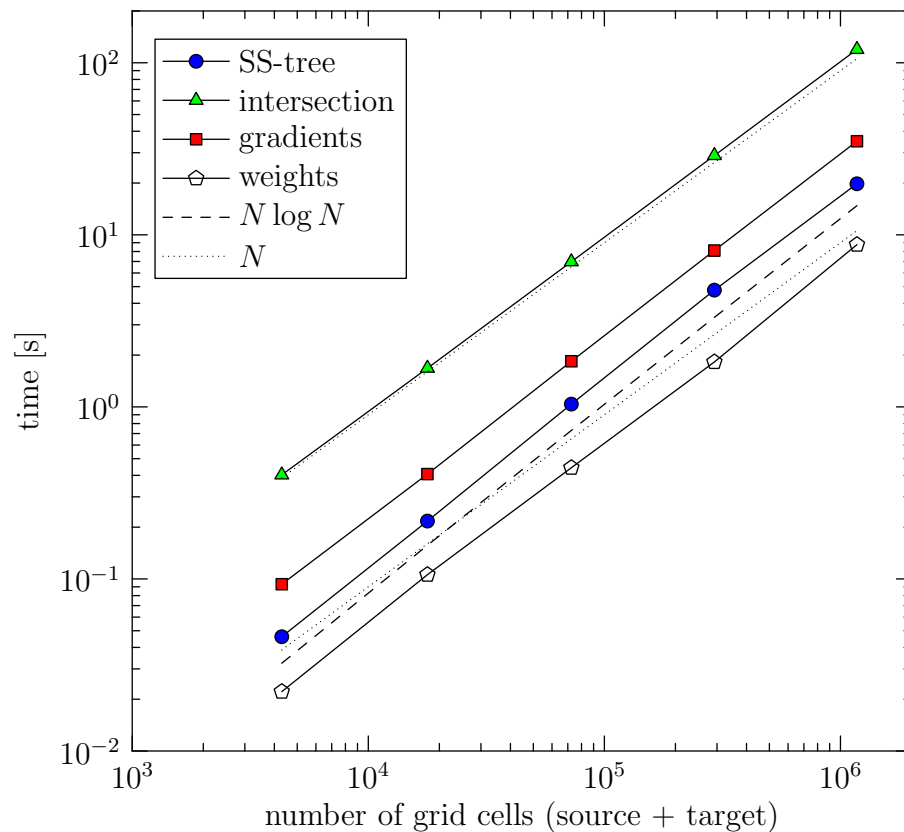


Figure 5. Timing of the various steps of second-order remapping from a uniform resolution icosahedral-hexagonal mesh to a regular latitude–longitude mesh. The SS-tree construction shows the expected $O(N \log N)$ complexity.